BIOCHEMISTRY
including biophysical chemistry & molecular biology

Article

pubs.acs.org/biochemistry

A Comparison of Three Fluorophores for the Detection of Amyloid Fibers and Prefibrillar Oligomeric Assemblies. ThT (Thioflavin T); ANS (1-Anilinonaphthalene-8-sulfonic Acid); and bisANS (4,4′-Dianilino-1,1′-binaphthyl-5,5′-disulfonic Acid)

Nadine D. Younan and John H. Viles*

School of Biological and Chemical Sciences, Queen Mary, University of London, Mile End Road, London E1 4NS, U.K.

Supporting Information

ABSTRACT: Amyloid fiber formation is a key event in many misfolding disorders. The ability to monitor the kinetics of fiber formation and other prefibrillar assemblies is therefore crucial for understanding these diseases. Here we compare three fluorescent probes for their ability to monitor fiber formation, ANS (1-anilinonaphthalene-8-sulfonic acid) and bis-ANS (4,4′-dianilino-1,1′-binaphthyl-5,5′-disulfonic acid) along with the more widely used thioflavin T (ThT). For this, we have used two highly amyloidogenic peptides: amyloid-β (Aβ) from Alzheimer's disease and islet amyloid polypeptide (IAPP) associated with type II diabetes. Using a well-plate reader, we show all three fluorophores can report the kinetics of fiber formation. Indeed, bis-ANS is markedly more sensitive to fiber detection than ThT and has a submicromolar affinity for Aβ fibers. Furthermore, we show that fluorescence detection is very sensitive to the presence of excess fluorophore. In particular, beyond a 1:1 stoichiometry these probes demonstrate marked fluorescence quenching, for both Aβ and IAPP. Indeed, the fiber-associated fluorescence signal is almost completely quenched in the presence of excess ThT. There is also intense interest in the detection of prefibrillar amyloid assemblies, as oligomers and protofibrils are believed to be highly cytotoxic. We generate stable, fiber-free, prefibrillar assemblies of Aβ and survey their fluorescence with ANS and bis-ANS. Fluorescence from ANS has often been used as a marker for oligomers; however, we show ANS can fluoresce more strongly in the presence of fibers and should therefore be used as a probe for oligomers with caution.

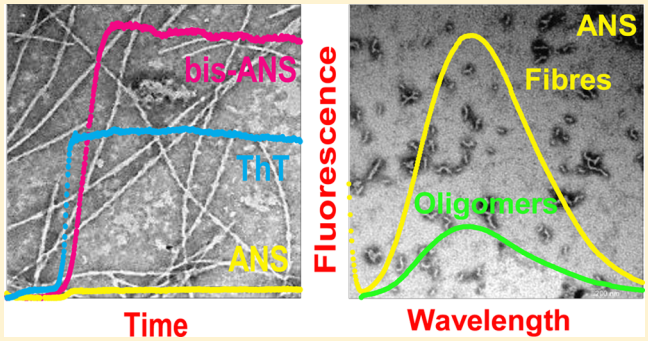

The self-assembly of various proteins into ordered oligomers and amyloid fibers is central to several protein misfolding disorders such as Alzheimer's and Parkinson's diseases and also transmissible spongiform encephalopathies and amyloid accumulation related to type II diabetes.[1] The amyloidogenicity or rate of fibril formation *in vitro* can often be related to the rate of disease onset. Furthermore, smaller cytotoxic oligomeric assemblies are thought to be the dominant toxic form in a number of misfolding diseases.[2,3] For this reason, the formation of oligomers and amyloid fibers, and their relationship, is the subject of much attention. The ability to detect amyloid fiber or oligomeric assemblies both *ex vivo* and *in vitro* is thought to be crucial to understanding the etiology of these diseases.

The most common technique for the detection of amyloid assemblies is to measure the fluorescence from noncovalently bound extrinsic fluorophores (reviewed in refs 4−7). *Ex vivo* tissue samples are commonly stained for amyloid deposits with thioflavin S (ThS) or Congo red,[8] while the thioflavin T (ThT) fluorophore is by far the most popular fluorescent probe used to detect fiber formation and growth kinetics *in vitro*.[9,10] The use of ThT as a fluorescent probe was first described in 1959 for the detection of amyloid rich tissue.[11,12] Key characteristics include the specificity of amyloid detection and an intense fluorescence signal and micromolar or submicromolar affinity for amyloid fibers.

It is generally believed the ThT molecules bind in the grooves along the surface of the amyloid fiber, running parallel to the long axis, created by the repeating arrangement of side chains on the surface of the cross-β structure.[7,13−16] The benzylamine and the benzathiole rings of ThT, when free in solution, will readily rotate about their central C−C bond (Figure 1). The low-energy nature of this rotation is thought to result in the quenching of the excited state of ThT's aromatic rings, which results in a minimal fluorescence signal. However, when ThT is bound to amyloid fibers, its freely rotating aromatic rings become fixed, leading to a marked increase in fluorescence.[13,17,18] ThT has some degree of specificity to

Received: March 20, 2015
Revised: June 17, 2015
Published: June 18, 2015

DOI: 10.1021/acs.biochem.5b00309
Biochemistry 2015, 54, 4297−4306

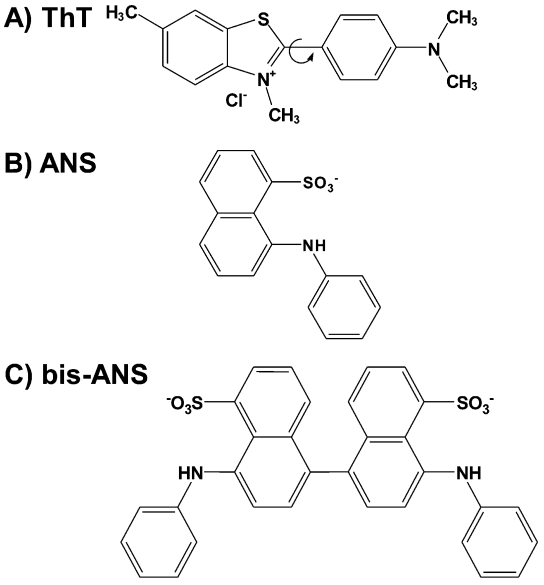

Figure 1. Chemical structures of the three fluorescent probes: thioflavin T (ThT), 8-anilinonaphthalene-1-sulfonate (ANS), and 4,4′-dianilino-1,1′-binaphthyl-5,5′-disulfonic acid (bis-ANS). The free rotation between the aromatic rings of ThT causes quenching of the fluorescence signal.

amyloid fibers; however, other hydrophobic patches can also give rise to ThT fluorescence; for example, the hydrophobic pockets within the all α-helical human serum albumin (HSA) cause some ThT fluorescence.[19] The dissociation constant of ThT for amyloid fibers is dependent on the pH and ionic strength and the protein amyloid investigated, leading to affinities for various amyloids ranging between dissociation constants of <0.1−64 μM (reviewed in refs 7 and 20).

Although they are much less commonly used and less well characterized, there have been some reports that have made use of other small fluorescent molecules to detect amyloid fibers and other prefibrillar states. It has been known for some time[21] that both 1-anilinonaphthalene-8-sulfonic acid (ANS)[22−27] and 4,4′-dianilino-1,1′-binaphthyl-5,5′-disulfonic acid (bis-ANS) (Figure 1)[4,24,28−35] fluoresce in the presence of fibers. However, the use of these dyes has not been directly compared with the use of ThT. Furthermore, their fluorescence properties when bound to fibers or their influence on fiber formation and structure have not been characterized in detail.

Prefibrillar oligomers and protofibrils are typically transient and heterogeneous structures that are often on the pathway to forming fibers.[30] Oligomers and protofibrils are thought to be the most cytotoxic for a number of protein misfolding diseases and are therefore of particular interest. However, a specific extrinsic fluorescent probe for these prefibrillar structures is less well established. ThT does not tend to fluoresce in the presence of prefibrillar assemblies; however, there are a few studies to suggest ANS is able to detect oligomers[28,29,36−38] and protofibrils.[39] We are not aware of any studies with bis-ANS and prefibrillar assemblies. If ANS or the related bis-ANS is to be a reliable probe for oligomer and protofibril assemblies, ideally they should give a fluorescent signal very distinct from that of amyloid fibers, as oligomeric assemblies are often a heterogeneous mixture with some fiber content.

Here we systematically compare the use of ANS and bis-ANS fluorescent dyes with the use of the commonly used ThT fluorophore for the measurement of the *in vitro* kinetics of amyloid fiber formation of Aβ, responsible for Alzheimer's disease, and islet amyloid polypeptide (IAPP), associated with type II diabetes. Furthermore, we compare the application of these three fluorophores for the detection of prefibrillar oligomeric and protofibril forms of Aβ by generating relatively stable, fiber-free assemblies. We aim to determine if bis-ANS and ANS are appropriate dyes for detection of oligomers and protofibers.

EXPERIMENTAL PROCEDURES

Peptide Production. All peptides were purchased from Generon or Cambridge Research Biochemicals, synthesized using Fmoc chemistry, purified as a single peak via high-performance liquid chromatography, and characterized by mass spectrometry. The purchased peptides included human amyloid-β peptide, residues 1−40 and 1−42 (designated Aβ_{40} and Aβ_{42}, respectively), and islet amyloid poly peptide (IAPP).

Peptide Sequences. Human Aβ(1−42): DAEFRHDSGY EVHHQKLVFF AEDVGSNKGA IIGLMVGGVV IA. Human IAPP(1−37): KCNTATCATQ RLANFLVHSS NNFGAILSST NVGSNTY.

Aβ Solubilization. Aβ_{40} or Aβ_{42} was solubilized at 0.7 mg/mL in water at pH 10.5 while being gently rocked at 4 °C for 48 h, and the pH was maintained at 10.5 using NaOH. This protocol has been found to be as effective or more effective than other solubilization protocols.[40,41] This process generated largely monomeric and seed-free Aβ_{40} stocks, based on nucleation times of many weeks, TEM images, and a lack of ThT fluorescence. After solubilization, the absorbance at 280 nm was used to calculate the concentration of Aβ, with an extinction coefficient of 1280 M^{-1} cm^{-1}.[42] The lyophilized peptide typically contains 10% water by weight.

IAPP Solubilization. IAPP was solubilized at a concentration of 3.56 mg/mL in 100% dimethyl sulfoxide (DMSO), and the peptide dissolved almost instantly. This method generates an essentially monomeric and seed-free IAPP stock. The absorbance signal at 280 nm was used to calculate the concentration of IAPP, with an extinction coefficient of 1400 M^{-1} cm^{-1}.[42] The final concentration of DMSO in the IAPP fiber growth assays did not exceed 2%.

Fiber Growth Kinetics. A solubilized stock of Aβ_{40} or Aβ_{42} and IAPP were typically diluted to 10 μM in 30 mM HEPES buffer (pH 7.4) with 160 mM NaCl and incubated at 30 °C. When the pH is lowered to 7.4, fiber formation will commence. The pH of a sample was monitored before and after each experiment, with a variation of ±0.05 pH unit or less observed over the course of the experiment. A fresh stock solution of ANS, bis-ANS, and ThT (Sigma-Aldrich) was dissolved in buffer. Typically, the fluorescent dye concentration ratio was 1:1 (dye:peptide) for ThT and bis-ANS or 2:1 (ANS:peptide).

The growth of fibers was monitored using a 96-well microplate plate BMG Omega FLUOstar fluorescence reader, with an excitation filter at 440 nm and an emission filter at 490 nm used to detect ThT, while an excitation filter at 355 nm and an emission filter at 520 nm were used for bis-ANS and ANS. Prior to each reading, the plate was agitated for 10−30 s via orbital (3 mm) shaking every 10−30 min. Sterile flat-bottom plates were used and sealed with Starseal polyolefin sealing film. The optimal well volume is 200 μL; these were used to their full capacity. Fluorescence detection was conducted using an orbital averaging sample reading (4 mm diameter).

Sigmoidal fibril growth curves are fitted to the following equation as previously described.[43]

DOI: 10.1021/acs.biochem.5b00309
Biochemistry 2015, 54, 4297−4306

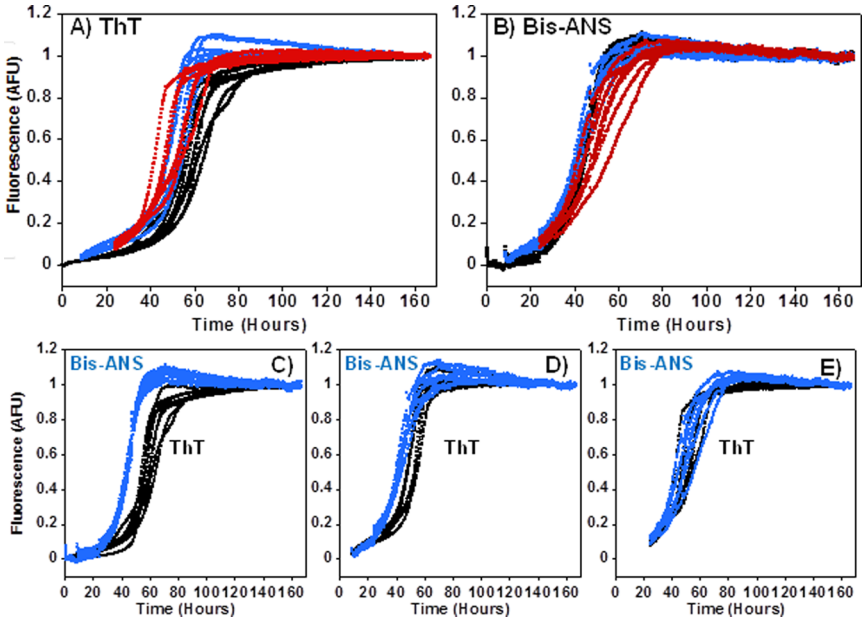

Figure 2. Comparison of Aβ_{42} fiber formation monitored by ThT and bis-ANS. The kinetics of Aβ_{42} fiber growth kinetics was monitored using two different fluorophores added at three different time points. Comparison of fiber kinetics in the presence of a fluorescent dye when added at 0 h (black), 8 h (blue), and 24 h (red): (A) 1 molar equiv of ThT and (B) 0.2 molar equiv of bis-ANS. Also, the effect of ThT (black) on fiber kinetics compared to that of bis-ANS (blue) at (C) 0 h, (D) 8 h, and (E) 24 h. The Aβ_{42} monomer (10 μM) was incubated at pH 7.4 in HEPES buffer (30 mM) and NaCl (160 mM) at 30 °C with intermittent agitation. The addition of fluorophores at different time points has little or no effect on the Aβ_{42} fiber formation kinetics.

$$Y = y_i + m_i x + \frac{v_f + m_f x}{1 + e^{-\left(\frac{X - X_o}{\tau}\right)}}$$

where Y is the fluorescence intensity, X is the time in hours, and X_o is the time at which the fluorescence has reached half-maximal intensity, also termed t_{50}. The apparent fiber growth rate (k_{app}) is calculated from the equation $k_{app} = 1/\tau$. The nucleation or lag time (t_{lag}) is taken from the equation $t_{lag} = X_o - 2\tau$.

Aβ_{42} Cu^{2+}-Induced Protofibrils and/or Oligomers. Cu^{2+}-induced protofibrils were prepared as previously described.[44] Essentially monomeric Aβ_{42} (10 μM) with 0.5 molar equiv of $CuCl_2$ was incubated at 30 °C in 160 mM NaCl with 30 mM HEPES (pH 7.5). Incubation for 5 days generates a stable oligomeric profibril; no fibrils were observed using TEM and ThT fluorescence.[44]

Aβ_{40} HFIP-Generated Oligomers. Aβ_{40} oligomers were prepared by dissolving 2.5 mg of peptide in 1 mL of 1,1,1,3,3,3-hexafluoroisopropanol (HFIP) and left at room temperature for 15 min as previously described.[45] A 10-fold dilution in water was then conducted, and the solution was incubated for a further 15 min at room temperature. The final solution was then centrifuged at 14000g for 15 min to remove any large aggregates.[45]

Transmission Electron Microscopy (TEM). Carbon-coated 300-mesh grids (SPI Supplies) were glow-discharged at the start of each experiment. An aliquot (5 μL) of the 10 μM Aβ sample was allowed to absorb onto a grid for 1 min before being blotted off. This step was then followed by a 5 μL aliquot of 2% (w/v) phosphotungstic acid (PTA), at pH 7.4, to be absorbed for 1 min, before blotting off to produce a negatively stained protein-loaded grid. Images of the grids were recorded on a JEOL JEM 1230 electron microscope operated at 80 kV.

Single-Cell Fluorescence Spectroscopy. Fluorescence emission spectra were recorded using a Hitachi F-2500 fluorescence spectrophotometer, in a 1 cm quartz cuvette (Hellma), using an excitation wavelength of 380 nm for ANS, 365 nm for bis-ANS, and 440 nm for ThT. Fluorescence emission was recorded between 400 and 600 nm.

RESULTS

Amyloid Fiber Detection and Fiber Growth Kinetics. We wanted to determine if bis-ANS and ANS, like ThT, could be used to monitor the kinetics of fiber formation. For this, we have used two peptides that readily form amyloid fibers: Aβ and IAPP. Using a fluorescent microplate reader, we directly compared the kinetics of fiber formation in the presence of the three fluorescent dyes. Bis-ANS and ANS readily detect amyloid fiber formation as is evident from the appearance of the sigmodal fiber growth curves that are similar to those observed for ThT fluorescence, shown in Figure 2, with characteristic nucleation, elongation, and equilibrium stages.

We considered the possibility that the fiber-detecting fluorophores might influence the rate of fibril formation. To investigate this, we monitored the kinetics by adding the fluorophores at different time points, as fibers were generated in the presence of bis-ANS and the widely used amyloid detection fluorophore, ThT. The nucleation time and the elongation rates were directly compared. If the fluorescent dye accelerates or inhibits fiber formation, the influence on the kinetics of fibril formation will be different when the dye is added at different time points. Figure 2 shows bis-ANS and ThT have little influence on the kinetics. The bis-ANS and ThT traces from three different time points (0, 8, and 21 h) all overlap; this is an indication that the nucleation phase and rate of Aβ_{42} fiber elongation are not significantly affected (Figure 2A,B). Importantly, this is irrespective of the time at which the fluorophore is added (Figure 2C–E).

DOI: 10.1021/acs.biochem.5b00309
Biochemistry 2015, 54, 4297–4306

It is possible that the fluorescent dyes might detect different Aβ assemblies; however, there is no evidence of either of the fluorophores, bis-ANS or ThT, detecting a transient prefibrillar species. For example, oligomers and protofibrills are thought to form before fibers but then become depleted as fibers are generated. It is clear that like in the case of ThT the bis-ANS is not selective for these transient species as there is no increase in fluorescence as protofibrils form, followed by a reduction or inflection in signal as fibers form.

Next, we investigated the effect of ANS on Aβ_{40} fiber growth kinetics. Here, the increasing concentrations of ThT and ANS did not affect the lag phase or the rate of fiber elongation (shown in Figure 3). A 10-fold increase in the amount of dye used did not affect the nucleation time.

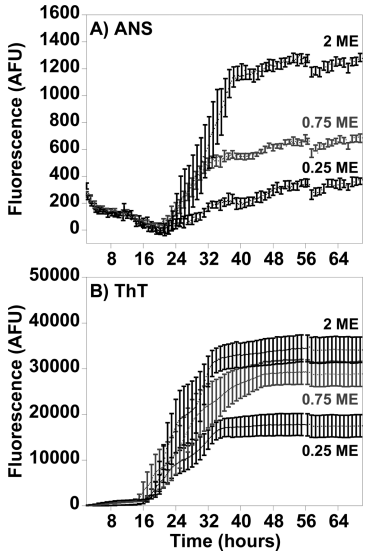

Figure 3. Comparison of Aβ_{40} fiber growth detection using ANS and ThT. Fiber growth kinetics of Aβ_{40} were studied using (A) ANS and (B) ThT. Aβ_{40} fiber growth was monitored at 0.25, 0.75, and 2 molar equiv to Aβ_{40} monomer (10 μM), incubated at pH 7.4 in HEPES buffer (30 mM) and NaCl (160 mM) at 30 °C with intermittent agitation. A 10-fold increase in dye concentration does not affect the fiber nucleation time.

We also used a second amyloid-forming system, IAPP, to probe the effect of the three fluorophores on fiber formation kinetics, in the presence of ThT, bis-ANS, and ANS (panels A–C of Figure 4, respectively). In the case of IAPP, there does appear to be a small but significant difference in the nucleation times depending on which fluorophore is used. Using the same stock solution of IAPP, nucleation times are 26 ± 5 min in the presences of ThT, and a similar lag time, 39 ± 4 min, for ANS is observed; however, for bis-ANS, the nucleation time is slower, 108 ± 2 min. Although the lag phase of IAPP fiber growth is affected depending on which dye is used, the elongation rates at which fibers grow are similar for all fluorophores, as shown Table 1.

Table 1. Fibril Growth Kinetics of IAPP in the Presence of Different Fluorophores[a]

	t_{50} (min)	t_{lag} (min)	k_{app} (min^{-1})	n
10 μM IAPP and 10 μM ThT	54 ± 4	26 ± 5	0.07 ± 0.01	10
10 μM IAPP and 20 μM ThT	45 ± 2	19 ± 4	0.08 ± 0.01	9
10 μM IAPP and 10 μM bis-ANS	132 ± 4	108 ± 2	0.1 ± 0.02	10
10 μM IAPP and 20 μM bis-ANS	115 ± 2	77 ± 3	0.06 ± 0.001	10
10 μM IAPP and 20 μM ANS	63 ± 4	39 ± 4	0.08 ± 0.002	10
10 μM IAPP and 40 μM ANS	56 ± 3	37 ± 4	0.11 ± 0.01	10

[a] n is the number of traces used in the analysis. Errors are shown as the mean standard error.

We wanted to determine if the amyloid fiber-detecting fluorophore had an appreciable influence on fibril morphology, as imaged by transmission electron microscopy (TEM). Figure 5 shows TEM images of Aβ_{42} fibers generated in the absence and presence of the three fluorophores, ThT, ANS, and bis-ANS. The presence of the dyes does not markedly affect the morphology of the Aβ_{42} fibers, according to the TEM images. The morphologies of Aβ_{42} fibers have the typical long unbranched appearance, ~10 nm thick, with twists in the fibers of regular periodicity.

Fluorescence Quenching at Higher Dye:Fiber Stoichiometries. With few studies using ANS and almost none using bis-ANS to detect fibers, we wanted to determine the most appropriate dye:amyloid protein stoichiometric ratio. Using preformed Aβ_{40} fibers, we loaded increasing levels of the dye onto the amyloid samples (Figure 6). With an Aβ_{40} concentration of 10 μM, increasing amounts of ThT, bis-

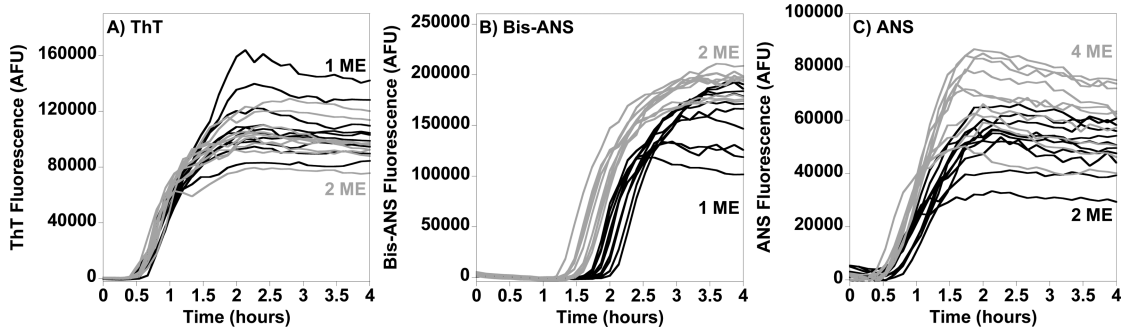

Figure 4. Influence of dyes on IAPP fiber growth kinetics. IAPP fibril growth was also monitored using ThT, ANS, and bis-ANS at two different concentrations. IAPP fiber formation was detected at 1 molar equiv (black) and 2 molar equiv (gray) of (A) ThT and (B) bis-ANS and 2 molar equiv (black) and 4 molar equiv (gray) of (C) ANS. The IAPP monomer (10 μM) was incubated at pH 7.4 in HEPES buffer (30 mM) and NaCl (160 mM) at 30 °C with intermittent agitation. ANS and ThT appear to accelerate fiber nucleation relative to bis-ANS.

DOI: 10.1021/acs.biochem.5b00309
Biochemistry 2015, 54, 4297–4306

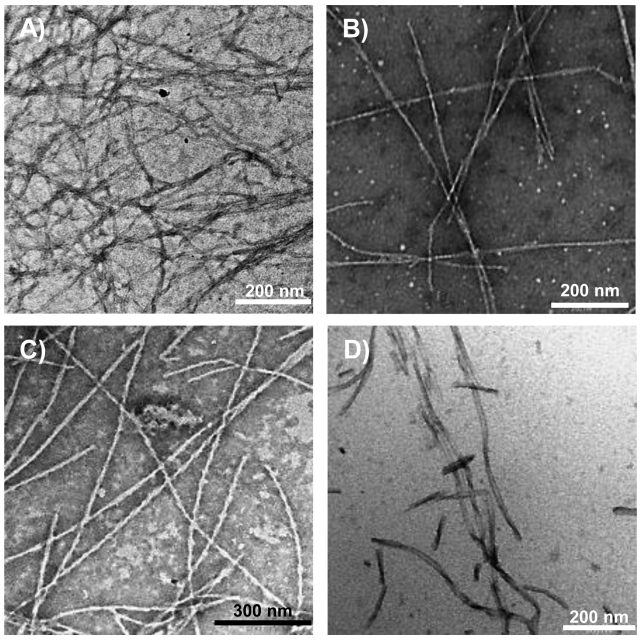

Figure 5. Effects of three different fluorophores on fiber morphology. The $A\beta_{42}$ fiber morphology was examined using negative stain transmission electron microscopy. $A\beta_{42}$ fibers grown (A) in the absence of a fluorescent probe and in the presence of (B) 1 molar equiv of ThT, (C) 0.2 molar equiv of bis-ANS, and (D) 2 molar equiv of ANS. $A\beta_{42}$ (10 μM) samples were incubated at pH 7.4 in 30 mM HEPES and 160 mM NaCl at 30 °C with intermittent agitation for 170 h.

ANS, and ANS (up to 10 molar equiv) were added. The ThT titration (Figure 6A) indicated that the fluorescence signal intensity increases linearly with increasing additions of ThT, up to 1 molar equiv. The fluorescence signal reaches a maximum at approximately 1 molar equiv, interestingly; concentrations of ThT beyond 1.5 molar equiv displayed a marked decrease in the intensity of the fluorescence signal. For example, by just 2 molar equiv, the intensity of ThT fluorescence was halved compared to its maximum, and by 10 molar equiv, there is only a tenth of the fluorescence signal left. It is clear that overly high suprastoichiometric levels of ThT, >2 molar equiv, will appreciably quench the fluorescence signal.

A very similar behavior is observed for bis-ANS (Figure 6C). As with ThT, excess bis-ANS also resulted in self-quenching; this is observed after 2 molar equiv of bis-ANS is added. This is highlighted in the bis-ANS titration (Figure 6D). At 4 molar equiv of bis-ANS, only half of the signal intensity, compared to the maximal signal, is observed. A similar titration with ANS was conducted (Figure 6E). Unlike those of the other two fluorophores, the ANS fluorescence intensity continues to grow beyond 1 molar equiv, although not linearly. Unlike bis-ANS and ThT, ANS exhibits little self-quenching up to 10 molar equiv (Figure 6F). Addition beyond 1 molar equiv of all three of the fluorophores causes a small shift in the maximal position of the fluorescence signal by 10 nm to longer wavelengths. We were surprised that excess ThT and bis-ANS caused such a marked quenching, so we repeated the experiment with $A\beta_{40}$ fibers with very similar results.

We were interested in whether the quenching effect of excess ThT was dependent on the stoichiometric ratio of ThT to Aβ (fiber) or the absolute concentration of ThT. We therefore repeated the experiment, but at 20 μM preformed Aβ fibers. The fluorescence behavior was very similar. The ThT fluorescence signal reaches a maximum close to 1 molar equiv (20 μM ThT) shown in Figure 7. Indeed, at 2 molar equiv (40 μM of ThT) the signal remains intense. With the lower Aβ fiber concentration 40 μM of ThT completely quenches the signal. The dominant factor in quenching is the ratio of dye to Aβ fiber rather than the total dye concentration.

Sensitivity and Affinity of the Fluorophore for Fiber Detection. *In vitro* detection of fiber formation can typically be achieved only at concentrations a number of orders of magnitude higher than physiological levels. It would be

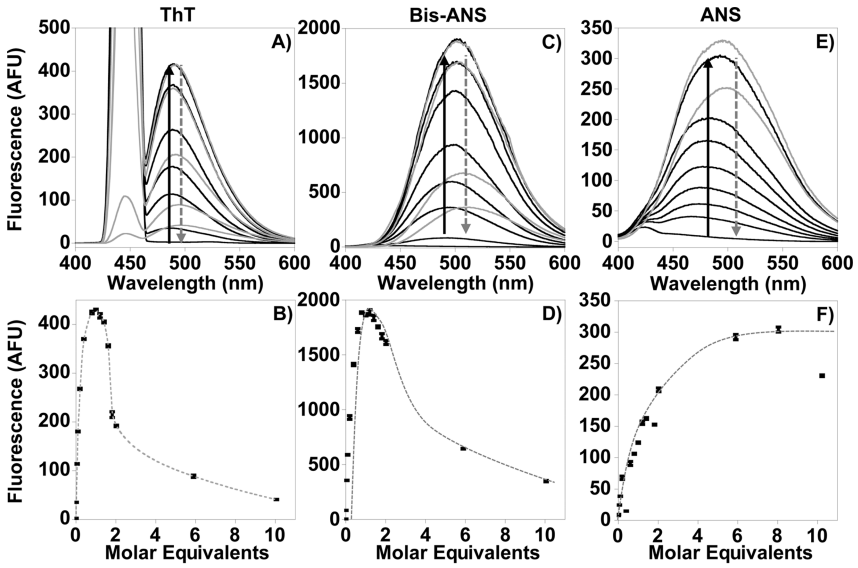

Figure 6. Excess fluorescent dye quenches the amyloid fiber-induced fluorescence. Using preformed $A\beta_{40}$ amyloid fibers, the titration of (A) ThT, (C) bis-ANS, and (E) ANS into a preformed $A\beta_{40}$ fiber sample. The increase in fluorescence (black) is represented by a solid upward-facing arrow, and the fluorescence self-quenching (gray) is represented by a dashed downward-facing arrow. The fluorescence intensity with increasing molar equivalents of dye is shown at (B) 489 nm for ThT, (D) 498 nm for bis-ANS, and (F) 480 nm for ANS. $A\beta_{40}$ fibers (10 μM) were preformed in 160 mM NaCl in the presence of 30 mM HEPES at pH 7.5.

DOI: 10.1021/acs.biochem.5b00309
Biochemistry 2015, 54, 4297−4306

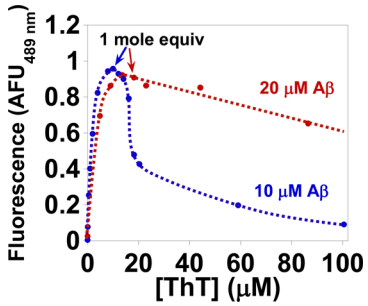

Figure 7. ThT fluorescence with increasing concentrations, in the presence of preformed Aβ_{40} fibers, at 10 μM Aβ_{40} fibers (blue) and 20 μM Aβ_{40} fibers (red). The maximal fluorescence is dependent on the stoichiometric ratio, not the total concentration of ThT. Aβ_{40} fibers were generated in 160 mM NaCl in the presence of 30 mM HEPES at pH 7.5 and 30 °C.

beneficial to have a fluorophore that can monitor fibers at lower concentrations. The ability to detect amyloid fibers by a fluorescent dye is dependent on the intensity of the fluorescence emitted, but also at the concentration at which the fluorescent probe has sufficient affinity to remain bound to the amyloid fiber. We wanted to compare the sensitivity of ThT, ANS, and bis-ANS to detect fibers. We took Aβ_{40} and also IAPP fibers and recorded the fluorescence signal in the presence of each dye, over a large range of concentrations (Figure 8). We monitored a serial dilution of a starting stock of Aβ_{40} fibers, 4.6 μM, in the presence of 1 molar equiv of ThT (Figure 7A). There is a linear relationship between the decrease in fluorescence and the reduction in Aβ_{40} fiber concentration. In addition, there is no shift in the wavelength of the fluorescence maxima. The behavior indicates that even at a low (0.3 μM) Aβ_{40} fiber concentration ThT is still tightly (fully) bound to the amyloid fiber. A lower concentration could not be measured because the signal fell below the fluorescence detection limit, defined here as 3 times the intensity of the background signal. The detection limit for which Aβ_{40} fibers will still produce a detectable fluorescence signal in the presence of 1 molar equiv of ThT is 0.3 μM. The bis-ANS fluorophore was also studied at a 1:1 ratio to Aβ_{40} fiber (Figure 8B). Much like ThT, bis-ANS remains fully bound to Aβ_{40} fibers even at low protein concentrations. The detection limit of bis-ANS is considerably lower, at 80 nM. These data indicate the affinity of bis-ANS for Aβ fibers has a dissociation constant tighter than ~80 nM.

To confirm the bis-ANS was still bound to Aβ_{40} at 100 nM, at equilibrium, we performed an additional experiment in which we added bis-ANS to a 100 nM fiber preparation, rather than dilute fibers with bis-ANS bound. As predicted for the data in Figure 8, bis-ANS can detect fibers at 100 nM Aβ (see Figure S1 of the Supporting Information).

The same dilution was performed for ANS bound to Aβ_{40} fibers. For ANS, 2 molar equiv of dye to Aβ_{40} fibers was used (the optimal ratio obtained from data shown in Figure 6). All three fluorophores show a close to linear relationship between fluorescence intensity and protein fiber concentration. As with the other fluorophores, ANS remains bound to Aβ_{40} fibers even at the lower concentrations, which is also indicated by the lack of a shift in the wavelength of the fluorescence maxima. ANS gives the weakest fluorescent signal; the detection limit for the ANS is 0.7 μM, which makes it considerably less sensitive than bis-ANS and ThT.

Fluorescent Probes for the Detection of Oligomeric and Protofibril Assemblies. Next we wanted to investigate the ability of ThT, bis-ANS, and ANS to detect other misfolded protein assemblies. To assess the fluorescent probes for the detection of prefibrillar assemblies, we generated stable homogeneous oligomers/protofibrils. These were generated for Aβ using two protocols. The first method involves Aβ_{42} in the presence of 0.5 molar equiv of Cu^{2+} ions,[44] and in the second method, the Aβ_{40} oligomers are generated using the solvent HFIP[45] (see Experimental Procedures). We chose these protocols to generate oligomers because assemblies are well-characterized and produce stable oligomers with no fibers present. HPIF-generated oligomers have been shown to disrupt long-term potentiation (LTP),[45] while Cu-Aβ_{42} has heightened cytotoxic activity[46] and disrupts the lipid bilayer.[44]

Stable Aβ oligomers/protofibrils generated in this way are visualized using TEM (Figure 9A,B). Figure 9 also shows the fluorescence spectra directly comparing all three fluorophores studied, for Aβ fibers and stable oligomers/protofibrils generated under the two different conditions (Cu^{2+} ions or HFIP). These fluorescence spectra were obtained with a 1:1 Aβ:fluorophore stoichiometry (or 1:2 for ANS) (Figure 9C–E). We compare fluorescence in the presence of the following: 10 μM Aβ_{40} fibers (represented by the orange trace), HFIP-prepared Aβ_{40} oligomers (green), and oligomers of 10 μM Aβ_{42} with 0.5 molar equiv of Cu^{2+} ions (purple). It is clear from

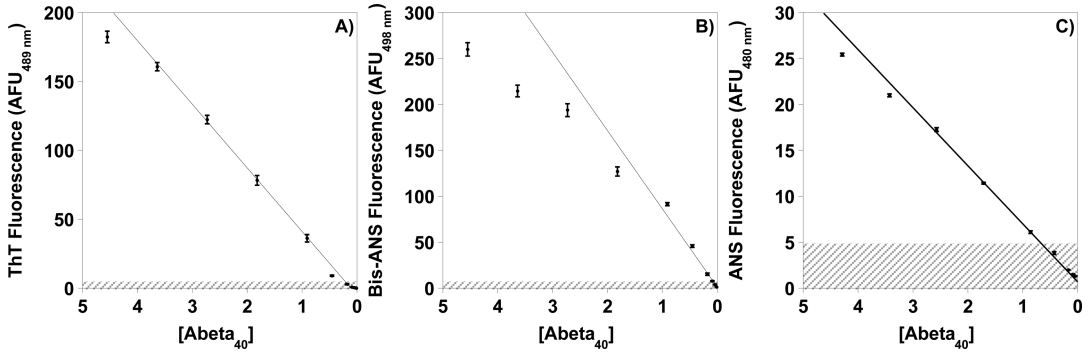

Figure 8. Detection limit for Aβ_{40} fibers using fluorescent probes. A serial dilution of Aβ_{40} in the presence of (A) 1 molar equiv of ThT, (B) 1 molar equiv of bis-ANS, and (C) 2 molar equiv of ANS was used to evaluate the detection limit. Aβ_{40} fibers (5 μM) were preformed in 160 mM NaCl in the presence of 30 mM HEPES at pH 7.5. The detection limit of the measurements was a fluorescence signal of 5 AFU represented as a gray dashed area.

DOI: 10.1021/acs.biochem.5b00309
Biochemistry 2015, 54, 4297–4306

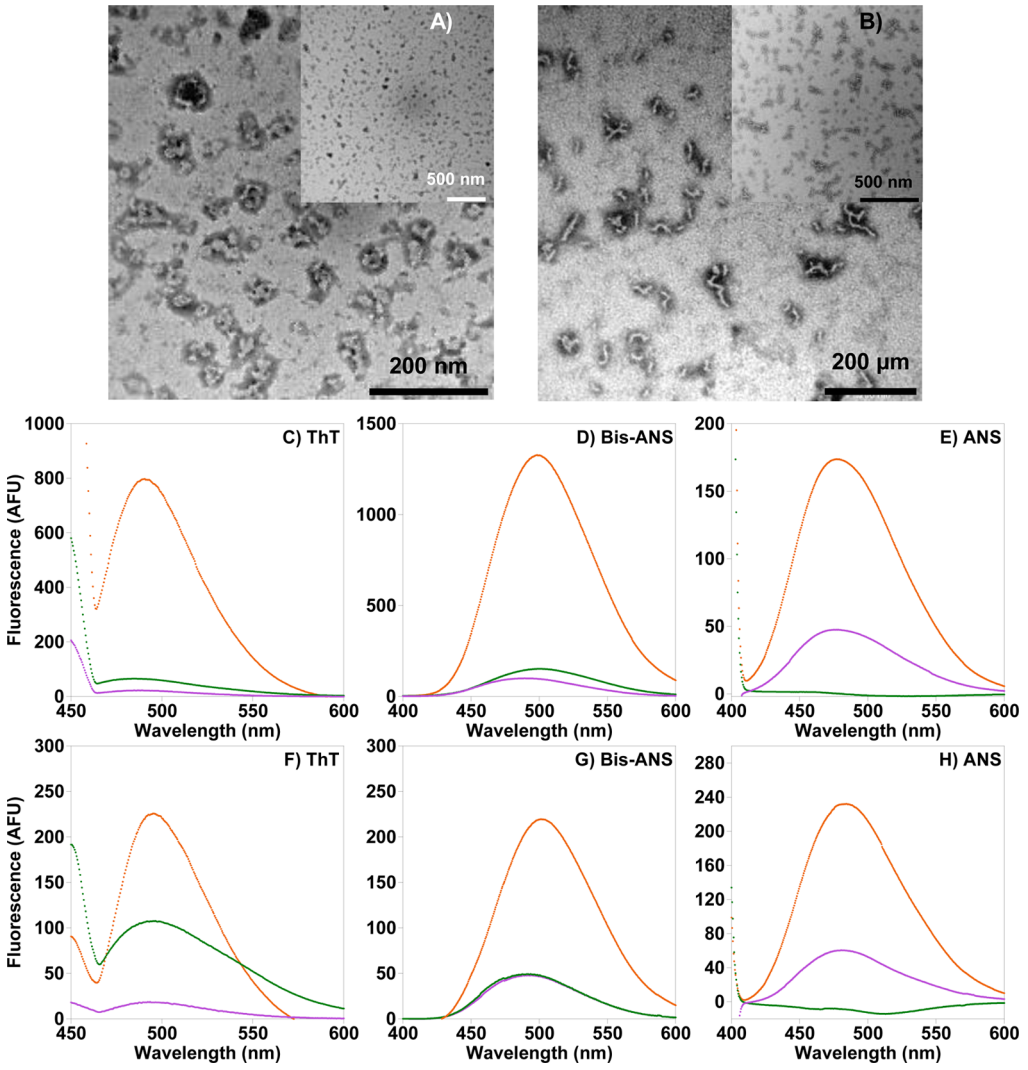

Figure 9. Comparison of ThT, bis-ANS, and ANS fluorescent signals in the presence of fibers and two oligomeric forms. TEM images of (A) HFIP-prepared Aβ_{40} oligomers and (B) Cu^{2+}-stabilized Aβ_{42} oligomers. Different structural assemblies of Aβ were used to test the specificity of the three fluorophores for fibers and oligomers at two different concentrations. Fluorescence signals of (C) 5 μM ThT, (D) 5 μM bis-ANS, (E) 10 μM ANS, (F) 50 μM ThT, (G) 50 μM bis-ANS, and (H) 50 μM ANS. Aβ_{40} fibers (orange), HFIP-generated Aβ_{40} oligomers (green), and Cu^{2+}-stabilized Aβ_{42} oligomers (purple) are all at a peptide concentration of 5 μM. All spectra have had the fluorescent signal for the dyes in water alone subtracted.

panels C and D of Figure 9 that only fibers are detected by a 1:1 level of ThT or bis-ANS. Indeed, these two dyes are very specific for fibers, and the fluorescent signal for both these oligomer/protofibrils is negligible and comparable to the signal generated in water alone (see Figure S2 of the Supporting Information). In contrast, ANS does generate some fluorescence signal for copper-Aβ_{42} oligomers/protofibrils, although it is not as intense as the signal observed for fibers.

There have been previous reports of ANS fluorescing in the presence of oligomers; typically, these experiments have been conducted with relatively large amounts of ANS (10:1).[29] We wondered if the high concentration of the fluorophore might detect oligomers and at the same concentration suppress the fluorescence signal from fibers. We therefore obtained fluorescence spectra for fibers and oligomers in the presence of 10 molar equiv of ANS, bis-ANS, and ThT. As expected, the fluorescence signal for fibers is markedly attenuated (by 75%) for both ThT and bis-ANS. Under conditions of excess ThT, the fluorescence signal for HFIP-generated oligomers is considerably more intense than that of background water. We note that for 10 molar equiv of bis-ANS and ANS the background fluorescence of the dye in water is more pronounced, especially relative to the substantially quenched fiber-induced fluorescence. Although fluorescence signals for the Aβ oligomers are observed, these signals are not substantially more intense than the background water signal for the dyes at 50 μM concentrations in water; furthermore, the wavelength maximum is also more indicative of the dye in water, as shown in Figure S2 of the Supporting Information.

The fluorophore 9-(2,2-dicyanovinyl) julolidine (DCVJ) has been proposed as a probe for prefibrillar oligomers;[4] however, our preliminary studies have shown no appreciable fluorescence for the prefibrillar oligomers and protofibrils described here.

DISCUSSION

Although there have been some reports of ANS and bis-ANS fluorescence in the presence of amyloid fibers,[4,21,23−28,30−35,47,48] often this fluorescence behavior with fibers is only briefly described. To the best of our knowledge, this is the first time bis-ANS and ANS have been used to

DOI: 10.1021/acs.biochem.5b00309
Biochemistry 2015, 54, 4297−4306

monitor the kinetics of amyloid fiber formation using a fluorescence well-plate reader together with direct comparison to ThT. It is clear that these fluorophores represent an excellent alternative to ThT when using well-plate fluorescence detection. ANS and bis-ANS are well-known for their significantly heightened fluorescence in the presence of molten globule protein conformations.[49] The mechanism by which bis-ANS and ANS fluorescence occurs in the presence of amyloid fibers presumably involves the binding of the dye to hydrophobic patches on the fiber, which results in a strong fluorescence signal.

Here we demonstrate that the lag and elongation phases of Aβ fiber formation are largely uninfluenced by bis-ANS or ANS. This is in line with other studies that have shown little effect on fiber growth rates in the presence of ThT.[5,50−52] However, this should not be assumed for all amyloid proteins. Fiber growth kinetics of IAPP indicate that bis-ANS binding and fluorescence are delayed relative to those of ThT and ANS. It appears bis-ANS can slow IAPP fiber nucleation.

The three dyes do not significantly affect fiber structure according to the TEM images. This might be expected as the amyloid fibers have to form before the fluorescent dye can bind with an appreciable affinity.

It is clear that amyloid fiber detection by ThT and bis-ANS is very sensitive to the ratio of dye to amyloid used. A small excess of dye can potentially drastically attenuate the fluorescent signal observed. Experimentalists should be aware of this when choosing the concentration of ThT or bis-ANS to detect fibers. The molar ratio that is optimal will depend on the structure of the particular amyloidogenic protein and the binding surface presented to the dye. It is evident that the use of excess ThT or bis-ANS dye can completely suppress the amyloid-dependent signal. An interesting consequence of these observations is that during the initial stages of fiber formation, when the total fiber content is low, the fluorescent signal may be quenched to an extent, delaying the appearance of the fiber-related fluorescence.

Previous studies have recommended that a 2:1 (ThT:Aβ) ratio should be used.[20] However, we suggest that for both Aβ and IAPP using ThT and bis-ANS at a 1:1 stoichiometry is more advisable. Excess ThT or bis-ANS, for example, 10 equiv, will significantly attenuate and quench the fluorescence signal, reducing the total fluorescence by 90% for Aβ. This effect was investigated at 10 and 20 μM Aβ (fibers). The stoichiometric ratio of ThT to Aβ fibers is the strongest determinant of the maximal fluorescent signal. It appears the reduction in the signal is not due to a simple internal filter effect. We speculate the quenching of ThT and bis-ANS fluorescence is due to weaker secondary binding of the fluorophore to the fiber−fluorophore complex, which induces static quenching. For ANS, a higher concentration of ANS versus that of Aβ is optimal. Two molar equivalents of ANS are required for efficient Aβ fiber detection.

In particular, if high sensitivity is important, bis-ANS represents an excellent alternative to ThT for monitoring fibers. When using a similar experimental protocol, the fluorescent signal (quantum yield) for bis-ANS is twice as intense as that of ThT and almost 20 times more sensitive than that of ANS. The linear relationship between Aβ_{40} fiber concentration and fluorescent signal intensity (for all three dyes), particularly at the dilute concentrations, indicates that the dye has an affinity for the Aβ_{40} fibers, which is sufficiently tight that the dye does not dissociate from the fiber even at the lower concentrations. This means the affinity of the dye for the fibers is tighter than the detection limit for these experiments. Bis-ANS therefore has a dissociation constant tighter than 80 nM, much tighter than the dissociation constant reported for ThT with a K_d of 2 μM at pH 6 reported for Aβ_{40},[20] although we note our data suggest the dissociation constant for ThT for Aβ_{40} is tighter than 500 nM at pH 7.4.

Oligomers and Protofibrils. Detection of prefibril oligomers and protofibrils is a vital objective for those wanting to characterize the role in toxicity for these assemblies.[30] A specific noncovalent fluorescent dye would have wide applications. There have been some studies reporting elevated fluorescence in the presence of ANS for prefibrillar oligomers.[28,29,37−39] Prefibrillar assemblies of Sup35 have been detected using Nile Red.[53] We are not aware of any studies with the related bis-ANS that characterize prefibrillar assemblies.

Thioflavin T is typically not thought to fluoresce in the presence of prefibrillar oligomers and protofibrils, and this is supported by our data for Cu^{2+}-generated protofibrils of Aβ_{42}. ThT does exhibit some fluorescence in the presence of HIPF-generated oligomers of Aβ_{40}; however, this is weak compared to the fluorescence observed for amyloid fibers and is observed with only 10 equiv of ThT present. Others have reported ThT fluorescence for oligomers of Aβ generated with the aid of prefoldin, a molecular chaperone.[38]

Bis-ANS appears to be the most selective of the three dyes for fibers only, as almost no fluorescence for both types of oligomers/profibrils studied here is detected. It is clear that unlike fibers, Aβ oligomers/profibrils generated here do not have a sufficiently large hydrophobic patch within them for bis-ANS to bind at micromolar concentrations.

On the other hand, ANS does give a fluorescence for the stable Aβ_{42} protofibrils generated in the presence of Cu^{2+} ions. These preparations are stable and contain minimal fiber content; indeed, the same sample gives no fluorescence in the presence of ThT or bis-ANS. This suggests that the ANS in contrast to the larger bis-ANS is able to bind to exposed hydrophobic patches within these protofibrils. However, it should not be assumed that the observation of ANS fluorescence is always an indication of oligomer formation, as ANS fluorescence may be considerable in the presence of a small subpopulation of fibers; therefore, the ANS fluorescence signal should be interpreted with caution. Indeed, ANS in water will give a small but detectable fluorescence, so when ANS is used at high concentrations, some of the fluorescence can be due to unbound background ANS fluorescence.

Bis-ANS and ANS give very strong fluorescence in partially folded molten globule structures. However, the oligomers/protofibrils described here do not exhibit similar fluorescence. It appears that any exposed hydrophobic patches on these oligomers do not provide a sufficiently large or tight binding site to induce applicable fluorescence and do not exhibit properties similar to those of molten globule structures. It is clear that a reliable alternative fluorescent probe to ANS for oligomer detection needs to be found.

In conclusion, bis-ANS is an excellent alternative to ThT for monitoring fiber formation kinetics *in vitro*. It produces a considerably more intense fluorescence signal in the presence of fibers than ThT and has a submicromolar affinity for Aβ amyloid fibers. In the case of Aβ or IAPP fibers, ThT and bis-ANS concentrations should not exceed a 1:1 molar stoichiometry to the monomer equivalent fiber concentration,

DOI: 10.1021/acs.biochem.5b00309
Biochemistry 2015, 54, 4297−4306

because both ThT and bis-ANS exhibit self-quenching of their fluorescence signal, and this will cause a considerable attenuation of the fluorescence signal. The use of stable, fiber-free, Aβ prefibrillar oligomeric preparations indicates that ANS can generate some fluorescence for Cu^{2+}-induced protofibrils of Aβ_{42}. We suggest the use of ANS to detect oligomers could be used in conjunction with bis-ANS to confirm the fluorescence signal is not from a subpopulation of fibers in the sample, as bis-ANS appears to be quite specific to fibers alone. The use of ANS as an extrinsic dye for oligomer detection is not ideal as ANS is also fluorescent in the presence of fibers. The identification of an oligomer specific dye is yet to be developed, although the combination of two fluorescence dyes with a FRET between them might be an approach to develop.[54]

■ ASSOCIATED CONTENT

Ⓢ Supporting Information

Fluorescence of bis-ANS for 100 nM Aβ_{40} fibers (Figure S1) and comparison of ThT, bis-ANS, and ANS fluorescent signals in the presence of fibers and two oligomeric forms (Figure S2). The Supporting Information is available free of charge on the ACS Publications website at DOI: 10.1021/acs.biochem.5b00309.

■ AUTHOR INFORMATION

Corresponding Author

*Telephone: 44-020-7882-8443. E-mail: j.viles@qmul.ac.uk.

Funding

This work was supported by Wellcome Trust Project Grant 093241/Z/10/Z.

Notes

The authors declare no competing financial interest.

■ ABBREVIATIONS

Aβ, amyloid-β peptide; ANS, 1-anilinonaphthalene-8-sulfonic acid; bis-ANS, 4,4′-dianilino-1,1′-binaphthyl-5,5′-disulfonic acid; DCVJ, 9-(2,2-dicyanovinyl) julolidine; HFIP, 1,1,1,3,3,3-hexafluoroisopropanol; IAPP, islet amyloid polypeptide; TEM, transmission electron microscopy; ThT, thioflavin T.

■ REFERENCES

(1) Stefani, M., and Dobson, C. (2003) Protein aggregation and aggregate toxicity: New insights into protein folding, misfolding diseases and biological evolution. *J. Mol. Med. 81*, 678−699.

(2) Lambert, M. P., Barlow, A., Chromy, B. A., Edwards, C., Freed, R., Liosatos, M., Morgan, T., Rozovsky, I., Trommer, B., and Viola, K. L. (1998) Diffusible, nonfibrillar ligands derived from Aβ1−42 are potent central nervous system neurotoxins. *Proc. Natl. Acad. Sci. U.S.A. 95*, 6448−6453.

(3) Walsh, D. M., Klyubin, I., Fadeeva, J. V., Cullen, W. K., Anwyl, R., Wolfe, M. S., Rowan, M. J., and Selkoe, D. J. (2002) Naturally secreted oligomers of amyloid β protein potently inhibit hippocampal long-term potentiation in vivo. *Nature 416*, 535−539.

(4) Lindgren, M., and Hammarström, P. (2010) Amyloid oligomers: Spectroscopic characterization of amyloidogenic protein states. *FEBS J. 277*, 1380−1388.

(5) Nielsen, L., Khurana, R., Coats, A., Frokjaer, S., Brange, J., Vyas, S., Uversky, V. N., and Fink, A. L. (2001) Effect of environmental factors on the kinetics of insulin fibril formation: Elucidation of the molecular mechanism. *Biochemistry 40*, 6036−6046.

(6) Hawe, A., Sutter, M., and Jiskoot, W. (2008) Extrinsic fluorescent dyes as tools for protein characterization. *Pharm. Res. 25*, 1487−1499.

(7) Groenning, M. (2010) Binding mode of Thioflavin T and other molecular probes in the context of amyloid fibrils: Current status. *J. Chem. Biol. 3*, 1−18.

(8) Westermark, G. T., Johnson, K. H., and Westermark, P. (1999) Characterization of in Vivo Protein Deposition: A. Identification and Isolation of Aggregates-1. Staining Methods for Identification of Amyloid in Tissue. *Methods Enzymol. 309*, 3−25.

(9) Levine, H., III (1997) Stopped-flow kinetics reveal multiple phases of thioflavin T binding to Alzheimer β (1−40) amyloid fibrils. *Arch. Biochem. Biophys. 342*, 306−316.

(10) Naiki, H., Higuchi, K., Hosokawa, M., and Takeda, T. (1989) Fluorometric determination of amyloid fibrils in vitro using the fluorescent dye, thioflavine T. *Anal. Biochem. 177*, 244−249.

(11) Vassar, P. S., and Culling, C. (1959) Fluorescent stains, with special reference to amyloid and connective tissues. *Arch. Pathol. 68*, 487.

(12) Saeed, S., and Fine, G. (1967) Thioflavin-T for amyloid detection. *Am. J. Clin. Pathol. 47*, 588.

(13) Biancalana, M., and Koide, S. (2010) Molecular mechanism of Thioflavin-T binding to amyloid fibrils. *Biochim. Biophys. Acta 1804*, 1405−1412.

(14) Krebs, M., Bromley, E., and Donald, A. (2005) The binding of thioflavin-T to amyloid fibrils: Localisation and implications. *J. Struct. Biol. 149*, 30−37.

(15) Biancalana, M., Makabe, K., Koide, A., and Koide, S. (2009) Molecular mechanism of thioflavin-T binding to the surface of β-rich peptide self-assemblies. *J. Mol. Biol. 385*, 1052−1063.

(16) Wu, C., Wang, Z., Lei, H., Duan, Y., Bowers, M. T., and Shea, J.-E. (2008) The Binding of Thioflavin T and Its Neutral Analog BTA-1 to Protofibrils of the Alzheimer's Disease Aβ_{16-22} Peptide Probed by Molecular Dynamics Simulations. *J. Mol. Biol. 384*, 718−729.

(17) Voropai, E., Samtsov, M., Kaplevskii, K., Maskevich, A., Stepuro, V., Povarova, O., Kuznetsova, I., Turoverov, K., Fink, A., and Uverskii, V. (2003) Spectral properties of thioflavin T and its complexes with amyloid fibrils. *J. Appl. Spectrosc. 70*, 868−874.

(18) Stsiapura, V. I., Maskevich, A. A., Kuzmitsky, V. A., Turoverov, K. K., and Kuznetsova, I. M. (2007) Computational study of thioflavin T torsional relaxation in the excited state. *J. Phys. Chem. A 111*, 4829−4835.

(19) Sen, P., Fatima, S., Ahmad, B., and Khan, R. H. (2009) Interactions of thioflavin T with serum albumins: Spectroscopic analyses. *Spectrochim. Acta, Part A 74*, 94−99.

(20) LeVine, H., III (1993) Thioflavine T interaction with synthetic Alzheimer's disease β-amyloid peptides: Detection of amyloid aggregation in solution. *Protein Sci. 2*, 404−410.

(21) LeVine, H. (2002) 4,4′-Dianilino-1,1′-binaphthyl-5,5′-disulfonite: Report on non-β-sheet conformers of Alzheimer's peptide β(1−40). *Arch. Biochem. Biophys. 404*, 106−115.

(22) Sarell, C. J., Woods, L. A., Su, Y., Debelouchina, G. T., Ashcroft, A. E., Griffin, R. G., Stockley, P. G., and Radford, S. E. (2013) Expanding the repertoire of amyloid polymorphs by co-polymerization of related protein precursors. *J. Biol. Chem. 288*, 7327−7337.

(23) Vetri, V., Canale, C., Relini, A., Librizzi, F., Militello, V., Gliozzi, A., and Leone, M. (2007) Amyloid fibrils formation and amorphous aggregation in concanavalin A. *Biophys. Chem. 125*, 184−190.

(24) Reinke, A. A., Seh, H. Y., and Gestwicki, J. E. (2009) A chemical screening approach reveals that indole fluorescence is quenched by pre-fibrillar but not fibrillar amyloid-β. *Bioorg. Med. Chem. Lett. 19*, 4952−4957.

(25) Koh, M., Lee, H., Lee, Y., and Lee, M. (2014) Characterization of early-stage amyloid aggregates by incorporating extrinsic fluorescence and atomic force microscopy. *J. Nanosci. Nanotechnol. 14*, 8386−8389.

(26) Li, M., Zhao, C., Yang, X., Ren, J., Xu, C., and Qu, X. (2013) In situ monitoring Alzheimer's disease β-amyloid aggregation and screening of Aβ inhibitors using a perylene probe. *Small 9*, 52−55.

(27) Goransson, A. L., Nilsson, K. P., Kagedal, K., and Brorsson, A. C. (2012) Identification of distinct physiochemical properties of toxic

DOI: 10.1021/acs.biochem.5b00309
Biochemistry 2015, 54, 4297−4306

prefibrillar species formed by Aβ peptide variants. *Biochem. Biophys. Res. Commun. 420*, 895−900.
(28) Lindgren, M., Sörgjerd, K., and Hammarström, P. (2005) Detection and characterization of aggregates, prefibrillar amyloidogenic oligomers, and protofibrils using fluorescence spectroscopy. *Biophys. J. 88*, 4200−4212.
(29) Bolognesi, B., Kumita, J. R., Barros, T. P., Esbjorner, E. K., Luheshi, L. M., Crowther, D. C., Wilson, M. R., Dobson, C. M., Favrin, G., and Yerbury, J. J. (2010) ANS binding reveals common features of cytotoxic amyloid species. *ACS Chem. Biol. 5*, 735−740.
(30) Fändrich, M. (2012) Oligomeric intermediates in amyloid formation: Structure determination and mechanisms of toxicity. *J. Mol. Biol. 421*, 427−440.
(31) Yu, M. F., Ryan, T. M., Ellis, S., Bush, A. I., Triccas, J. A., Rutledge, P. J., and Todd, M. H. (2014) Neuroprotective peptide-macrocycle conjugates reveal complex structure-activity relationships in their interactions with amyloid β. *Metallomics 6*, 1931−1940.
(32) Carnini, A., Lear, J. D., and Eckenhoff, R. G. (2007) Inhaled anesthetic modulation of amyloid β(1−40) assembly and growth. *Curr. Alzheimer Res. 4*, 233−241.
(33) LeVine, H. (2006) Biotin-avidin interaction-based screening assay for Alzheimer's β-peptide oligomer inhibitors. *Anal. Biochem. 356*, 265−272.
(34) Ferrao-Gonzales, A. D., Robbs, B. K., Moreau, V. H., Ferreira, A., Juliano, L., Valente, A. P., Almeida, F. C. L., Silva, J. L., and Foguel, D. (2005) Controlling β-amyloid oligomerization by the use of naphthalene sulfonates: Trapping low molecular weight oligomeric species. *J. Biol. Chem. 280*, 34747−34754.
(35) Kremer, J. J., Pallitto, M. M., Sklansky, D. J., and Murphy, R. M. (2000) Correlation of β-amyloid aggregate size and hydrophobicity with decreased bilayer fluidity of model membranes. *Biochemistry 39*, 10309−10318.
(36) Frare, E., Mossuto, M. F., de Laureto, P. P., Tolin, S., Menzer, L., Dumoulin, M., Dobson, C. M., and Fontana, A. (2009) Characterization of oligomeric species on the aggregation pathway of human lysozyme. *J. Mol. Biol. 387*, 17−27.
(37) Göransson, A.-L., Nilsson, K. P. R., Kågedal, K., and Brorsson, A.-C. (2012) Identification of distinct physiochemical properties of toxic prefibrillar species formed by Aβ peptide variants. *Biochem. Biophys. Res. Commun. 420*, 895−900.
(38) Sakono, M., Zako, T., Ueda, H., Yohda, M., and Maeda, M. (2008) Formation of highly toxic soluble amyloid β oligomers by the molecular chaperone prefoldin. *FEBS J. 275*, 5982−5993.
(39) Dubnovitsky, A., Sandberg, A., Rahman, M. M., Benilova, I., Lendel, C., and Hard, T. (2013) Amyloid-β protofibrils: Size, morphology and synaptotoxicity of an engineered mimic. *PLoS One 8*, e66101.
(40) Fezoui, Y., Hartley, D. M., Harper, J. D., Khurana, R., Walsh, D. M., Condron, M. M., Selkoe, D. J., Lansbury, P. T., Jr., Fink, A. L., and Teplow, D. B. (2000) An improved method of preparing the amyloid β-protein for fibrillogenesis and neurotoxicity experiments. *Amyloid 7*, 166−178.
(41) Teplow, D. B. (2006) Preparation of amyloid β-protein for structural and functional studies. *Methods Enzymol. 413*, 20−33.
(42) Gill, S. C., and von Hippel, P. H. (1989) Calculation of protein extinction coefficients from amino acid sequence data. *Anal. Biochem. 182*, 319−326.
(43) Uversky, V. N., Li, J., and Fink, A. L. (2001) Metal-triggered structural transformations, aggregation, and fibrillation of human α-synuclein. *J. Biol. Chem. 276*, 44284.
(44) Matheou, C. J., Younan, N. D., and Viles, J. H. (2015) Cu^{2+} accentuates distinct misfolding for Aβ(1−40) and Aβ(1−42) peptides, and potentiates membrane disruption. *Biochem. J. 466*, 233−242.
(45) Haupt, C., Leppert, J., Rönicke, R., Meinhardt, J., Yadav, J. K., Ramachandran, R., Ohlenschläger, O., Reymann, K. G., Görlach, M., and Fändrich, M. (2012) Structural Basis of β-Amyloid-Dependent Synaptic Dysfunctions. *Angew. Chem., Int. Ed. 51*, 1576−1579.
(46) Sarell, C. J., Wilkinson, S. R., and Viles, J. H. (2010) Substoichiometric levels of Cu^{2+} ions accelerate the kinetics of fiber formation and promote cell toxicity of amyloid-β from Alzheimer disease. *J. Biol. Chem. 285*, 41533−41540.
(47) Sarell, C. J., Woods, L. A., Su, Y., Debelouchina, G. T., Ashcroft, A. E., Griffin, R. G., Stockley, P. G., and Radford, S. E. (2013) Expanding the repertoire of amyloid polymorphs by co-polymerization of related protein precursors. *J. Biol. Chem. 288*, 7327−7337.
(48) Bolognesi, B., Kumita, J. R., Barros, T. P., Esbjorner, E. K., Luheshi, L. M., Crowther, D. C., Wilson, M. R., Dobson, C. M., Favrin, G., and Yerbury, J. J. (2010) ANS binding reveals common features of cytotoxic amyloid species. *ACS Chem. Biol. 5*, 735−740.
(49) Goto, Y., and Fink, A. L. (1989) Conformational states in β-lactamase: Molten-globule states at acidic and alkaline pH with high salt. *Biochemistry 28*, 945−952.
(50) Foderà, V., Librizzi, F., Groenning, M., Van De Weert, M., and Leone, M. (2008) Secondary nucleation and accessible surface in insulin amyloid fibril formation. *J. Phys. Chem. B 112*, 3853−3858.
(51) Chander, H., Chauhan, A., and Chauhan, V. (2007) Binding of Proteases to Fibrillar Amyloid-β Protein and its Inhibition by Congo Red. *J. Alzheimer's Dis. 12*, 261−269.
(52) Manno, M., Craparo, E. F., Podestà, A., Bulone, D., Carrotta, R., Martorana, V., Tiana, G., and San Biagio, P. L. (2007) Kinetics of different processes in human insulin amyloid formation. *J. Mol. Biol. 366*, 258−274.
(53) Krishnan, R., Goodman, J. L., Mukhopadhyay, S., Pacheco, C. D., Lemke, E. A., Deniz, A. A., and Lindquist, S. (2012) Conserved features of intermediates in amyloid assembly determine their benign or toxic states. *Proc. Natl. Acad. Sci. U.S.A. 109*, 11172−11177.
(54) Alies, B., Eury, H., Essassi, E. M., Pratviel, G., Hureau, C., and Faller, P. (2014) Concept for Simultaneous and Specific in Situ Monitoring of Amyloid Oligomers and Fibrils via Förster Resonance Energy Transfer. *Anal. Chem. 86*, 11877−11882.

DOI: 10.1021/acs.biochem.5b00309
Biochemistry 2015, 54, 4297−4306